Probing the Pu^{4+} magnetic moment in PuF_4 with ^{19}F NMR spectroscopy

Cigdem Capan,[1] Richard J. Dempsey,[1] Sergey Sinkov,[2] Bruce K. McNamara,[2] and Herman Cho[3,*]

[1]*Washington State University, Richland, Washington 99352, USA*

[2]*Energy and Environmental Directorate, P.O. Box 999, Pacific Northwest National Laboratory, Richland, Washington 99352, USA*

[3]*Physical and Computational Sciences Directorate, P.O. Box 999, Pacific Northwest National Laboratory, Richland, Washington 99352, USA*

(Received 15 April 2016; revised manuscript received 18 May 2016; published 8 June 2016)

The magnetic fields produced by Pu^{4+} centers have been measured by ^{19}F NMR spectroscopy to elucidate the Pu-F electronic interactions in polycrystalline PuF_4. Spectra acquired at applied fields of 2.35 and 7.05 T reveal a linear scaling of the ^{19}F line shape. A model is presented that treats the line broadening and shifts as due to dipolar fields produced by Pu valence electrons in localized noninteracting orbitals. Alternative explanations for the observed line shape involving covalent Pu-F bonding, superexchange interactions, and electronic configurations with enhanced magnetic moments are considered.

DOI: 10.1103/PhysRevB.93.224409

I. INTRODUCTION

Soon after the synthesis of the first transuranic elements, Seaborg proposed that the actinide elements were $5f$ analogs of the lanthanide ($4f$) series, as implied by the placement of the actinide row below the lanthanide row in the periodic table [1]. Heavy actinides have indeed been found to behave similarly to the lanthanides, but at plutonium there is a discontinuity whereupon lighter actinide elements exhibit physical and chemical properties more closely associated with transition metals [2–4]. These trends suggest that Pu is the pivotal element to study for insights on the electronic structure of the actinide series.

Valence electrons in $4f$ and $5f$ shells, unlike lower angular momentum orbitals, may display atomic ("localized") or bandlike ("itinerant") character depending on the degree of hybridization with electrons of neighboring atoms. This duality underlies many phenomena unique to lanthanide and actinide compounds such as extremely slow conduction electrons with large mass renormalization ("heavy fermions") [5], unusual quadrupolar (or higher) magnetic ordering [6], and unconventional superconductivity [7–10]. The complexity of the electronic structure of Pu is illustrated by a recent study of δ-Pu, wherein a theory involving a novel fluctuating valence ground state was developed to describe the lack of magnetism [11].

To better understand the behavior of electrons in Pu, comparisons of compounds with isostructural lanthanide counterparts are instructive. One such system is PuF_4 [12,13], which has both lanthanide and other actinide analogs [14]. In spite of their simple stoichiometry, actinide tetrafluorides AnF_4 exemplify the difficulties of relating f-electron configurations to observed properties. The metal is coordinated to eight fluorine atoms in the structure of the tetrafluoride compounds (Fig. 1), and thus these cannot be straightforwardly portrayed as a lattice formed by ions with formal charges $(An^{4+})(F^{-})_4$. The number of electrons per unit cell is even, suggesting that PuF_4 is a band insulator, but to our knowledge this prediction has not been confirmed. Previous magnetic susceptibility measurements indicate a paramagnetic system consistent with a $5f^4$ configuration [15]. Specific heat data reveal no sign of ordering down to 10 K [16], despite a substantial antiferromagnetic coupling among the Pu moments, as evidenced by the Curie-Weiss temperature of $\Theta = 290$ K [15]. X-ray photoelectron spectroscopy measurements in isostructural UF_4 showed some covalent character for the f electrons [17] even though the magnetic susceptibility obeys Curie-Weiss behavior consistent with local moment paramagnetism [18].

The possibility of probing f electrons through their interactions with nuclear spins makes nuclear magnetic resonance spectroscopy (NMR) an appealing approach for investigating the magnetism of actinide compounds. While NMR investigations in strongly correlated electron materials often focus on the temperature dependence of Knight shifts and relaxation times [19], line shapes of NMR signals from ligand nuclei can also be used to infer details on the electronic configuration of paramagnetic metal centers surrounding the ligand [20]. Actinide and lanthanide tetrafluorides, with their high density of the NMR-favorable ^{19}F isotope, are attractive for such experiments.

II. EXPERIMENTAL

A. Sample description

The PuF_4 sample used here was drawn from a stock of powder produced at the U.S. Department of Energy's Hanford Site Plutonium Finishing Plant [21]. Plutonium and americium isotope contents were measured in triplicate by thermal ionization mass spectrometry and gamma spectrum analysis (Table I). The NMR sample (mass = 581 mg) was doubly contained in robust nested capsules made with PEEK (OD = 7.5 mm). The ^{19}F NMR background of the PEEK capsules was negligible in comparison to the PuF_4 signal. Caution: Plutonium-239 is an alpha emitter (specific activity $= 2.30 \times 10^9$ Bq/g) that presents both radioactivity and toxicity hazards. All sample manipulations were performed in the Radiochemical Processing Laboratory, which is a U.S. Department of Energy category 2 nuclear facility located at the Pacific Northwest National Laboratory.

B. Spectroscopy

Data were acquired at ambient temperatures with 2.35 and 7.05 T superconducting magnets, corresponding to ^{19}F

*hm.cho@pnnl.gov

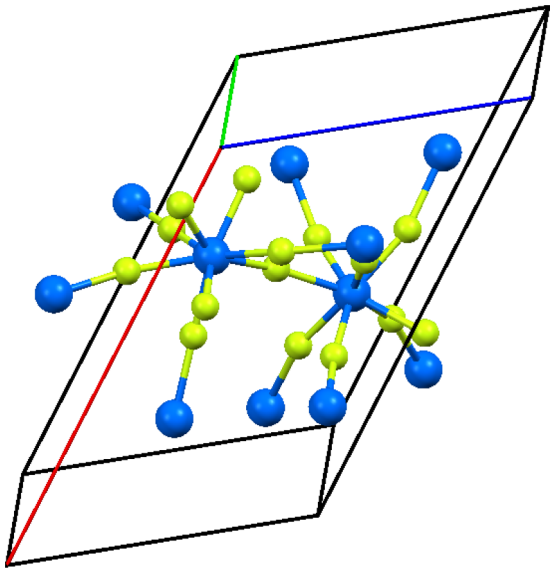

FIG. 1. Monoclinic crystal structure of PuF_4 illustrating the coordination of Pu (blue) with eight fluorine atoms (green) and the near linearity of the Pu-F-Pu bridges.

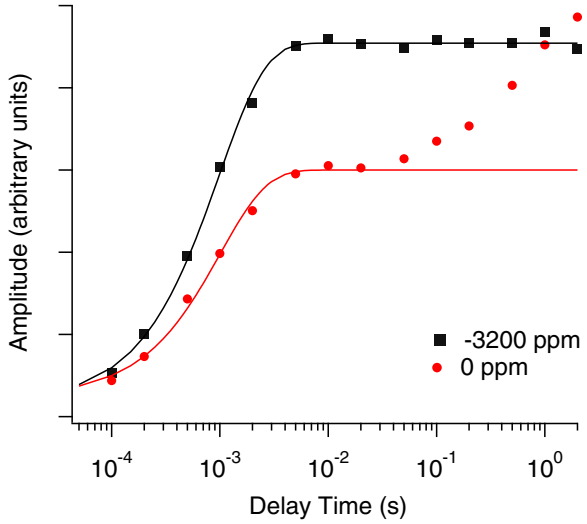

FIG. 2. Integrated ^{19}F NMR signal intensities vs delay time for PuF_4 measured at 2.35 T. Measurements at the two indicated frequencies in the inhomogeneously broadened line shape are shown, along with fits to a single-exponential recovery function.

Larmor frequencies of 93.62 and 282.41 MHz, respectively. Both instruments were equipped with Redstone consoles from Tecmag, Inc. The ^{19}F NMR frequency scale was referenced with 0.01 M NaF dissolved in 1.0 M $NaClO_4$(aq) at room temperature [22]. Radio frequency (rf) field amplitudes (B_1) were calibrated with nutation experiments on a concentrated NaF(aq) solution.

A two-pulse solid echo experiment [23] and a 16 step phase cycle [24] were used to detect the PuF_4 ^{19}F signal. Refocusing times for the echo were 8–12 μs. The inhomogeneously broadened PuF_4 ^{19}F resonance was recorded in a piecewise fashion by stepping the spectrometer carrier frequency across the entire spectral region. The signal intensity at each frequency was obtained by integrating the Fourier transform of the echo signal. The output of the rf amplifier was monitored and adjusted as needed to provide a constant field amplitude at each frequency step of the spectrum. The spectrum was measured with several B_1 field amplitudes ranging between 0.1 to 0.9 mT in the rotating frame. Signal intensities were greater with increased B_1 fields, but the overall line shape was unchanged, and no sign of power broadening was observed.

Spin-lattice relaxation times (T_1) were determined by the saturation recovery method. Figure 2 shows the integrated NMR signal intensity as a function of the magnetization recovery time, measured in the 2.35 T field. A two-step recovery is observed. A slow recovery signal appears within a 200 kHz range around the ^{19}F Larmor frequency, and can be assigned to diamagnetic fluorinated parts in the housing and circuit of the probe. The T_1 of this signal was found to be more than 100 times longer than the T_1 ($\sim$1 ms) of the second relaxation process, which we assign to PuF_4. The measured relaxation time of PuF_4 varied by less than 14% over the entire frequency range and was found to be the same at both fields. Because of the disparity in relaxation times, the background signal could be selectively attenuated by applying a saturating pulse train and delaying acquisition of the echo transient by a time long compared to the PuF_4 T_1 but short relative to the background signal recovery time.

TABLE I. Plutonium isotope distribution in the PuF_4 NMR sample. The ^{241}Am content was found by gamma spectral analysis to be 0.0050 m/m relative to ^{239}Pu.

	Mass fraction normalized to total Pu	
Isotope	GEA[a]	TIMS[b]
^{238}Pu	ND[c]	0.0001
^{239}Pu	0.9339	0.9416
^{240}Pu	0.0656	0.0576
^{241}Pu	0.0004	0.0005
^{242}Pu	ND[c]	0.0002

[a]GEA: gamma energy analysis.
[b]TIMS: thermal ionization mass spectrometry.
[c]ND: not detected.

III. RESULTS AND DISCUSSION

Fluorine-19 NMR spectra acquired in a stepped frequency mode as described above appear in Fig. 3. Spectral data are presented in accordance with the recommendation of the IUPAC [25], which specifies line positions in terms of a scaled shift from the signal of a reference compound:

$$\delta = \frac{\nu - \nu_R}{\nu_R} \times 10^6 = \frac{\sigma_R - \sigma}{1 - \sigma_R} \times 10^6, \quad (1)$$

where ν and ν_R represent the NMR frequencies of the sample and reference nuclei, respectively, and σ refers to the absolute shielding parameter (in ppm). The position of the ^{19}F resonance of hydrated F^- on the shift scale having $CFCl_3$ as the reference compound is -125.0 ppm [26].

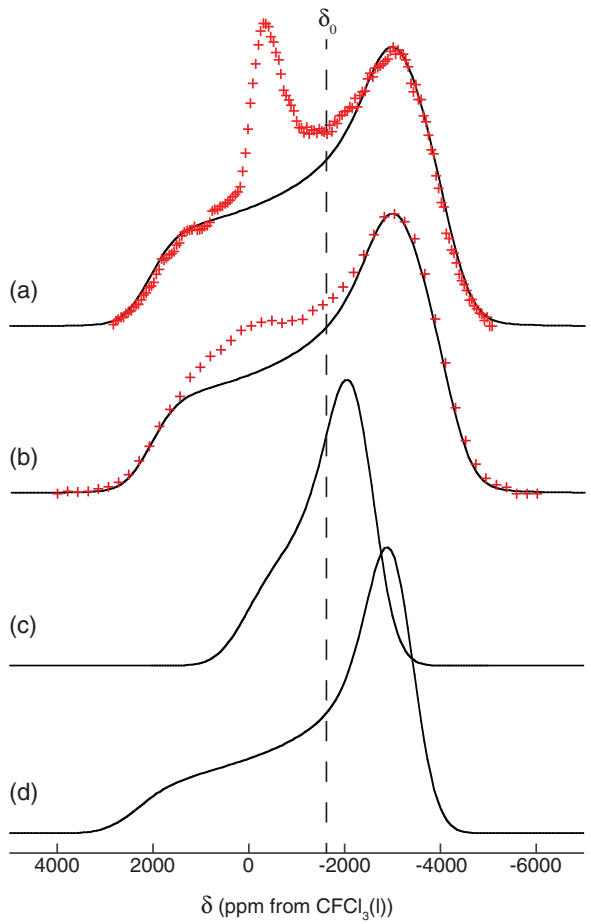

FIG. 3. Fluorine-19 spectra of PuF_4(s). Experimental spectral intensities were measured as a function of the spectrometer carrier frequency at magnetic fields of 7.05 T (a) and 2.35 T (b), and are indicated by red crosses. Solid curves in (a) and (b) are fits of the function in Eq. (2) to the experimental data; nonfitted features centered at ∼0 ppm are from residual ^{19}F background signal. Simulated spectra were computed with models that assume $5f^4$ (c) and $5f^3\,6d^1$ (d) Pu electronic configurations (*vide infra*); these spectra have been centered at the same isotropic shift frequency as (a) and (b) ($\delta_0 = -1620$ ppm) symbolized by the dashed line. Note that at fixed field, energy increases from right to left on the δ scale.

The anisotropic local magnetic fields giving rise to the experimental spectra in Fig. 3 were modeled by a second rank Cartesian tensor with principal values δ_{xx},δ_{yy}, and δ_{zz}, which are proportional to the applied field and can be extracted from the ^{19}F line shapes by fitting the experimental points to the function [27,28]

$$\delta = \delta_0 + \tfrac{1}{2}\delta_1[(3\cos^2\theta - 1) - \eta\sin^2\theta\cos 2\phi], \qquad (2)$$

where δ_0,δ_1, and η are defined according to the standard expressions

$$\delta_0 \equiv \tfrac{1}{3}(\delta_{xx} + \delta_{yy} + \delta_{zz}),$$
$$\delta_1 \equiv \delta_{zz} - \delta_0,$$
$$\eta \equiv \frac{\delta_{yy} - \delta_{xx}}{\delta_1},$$

TABLE II. Fitted shift parameters for PuF_4 ^{19}F spectra. Spectra calculated with the nonaxial tensor appear in Figs. 3(a) and 3(b). The model spectra were convolved with a Gaussian function (FWHM = 1100 ppm) as part of the fitting process.

	ppm from $CFCl_3$(l)			
	δ_{xx}	δ_{yy}	δ_{zz}	η
Axial	−3489	−3489	2118	0.00
Nonaxial	−4078	−2900	2118	0.32

with $|\delta_{zz} - \delta_0| \geqslant |\delta_{xx} - \delta_0| \geqslant |\delta_{yy} - \delta_0|$, and θ and ϕ are the longitudinal and azimuthal angles, respectively, describing the orientation of the principal axis system of the tensor with respect to the applied field $\mathbf{B}_0$. The δ_{jj} obtained from the fit of Eq. (2) to the experimental data appear in Table II. Two fits were performed, one in which δ_{xx},δ_{yy}, and δ_{zz} were allowed to vary freely, and another in which the shift tensor was forced to be axially symmetric as proposed by Gabuda *et al.* for the isostructural compound UF_4 [29]. The nonaxial function was statistically superior to the axial function in modeling the spectra, even accounting for the extra adjustable parameter in the former. A spectrum comparable in appearance and slightly narrower in width has been observed for UF_4 (∼3 mT, corresponding to 4920 ppm) [29].

Absolute shielding parameters can be ascertained from the shifts in Table II using data from Hindermann and Cornell, who reported a value of $\sigma_0 = +188.7$ ppm for liquid $CFCl_3$ based on a calculated shielding of $\sigma_0 = +410.0$ ppm for HF(g) [30,31]. The principal values of the shielding tensor computed in this way from the nonaxial shift tensor are (in ppm) $(\sigma_{xx},\sigma_{yy},\sigma_{zz}) = (4267,3089,-1929)$; adjustments can be readily made through addition or subtraction of a constant offset as improved estimates of $\sigma_0(CFCl_3)$ become available [32].

The shifts and line shapes of the observed spectra in Fig. 3 are determined by the cumulative effects of ^{19}F-^{19}F dipolar couplings, the chemical shift, and hyperfine couplings to unpaired electrons at the metal. The contribution of the homonuclear dipolar interaction to the ^{19}F line width was evaluated using C^{++} computer programs written with object code from the GAMMA simulation environment [33]. These calculations reveal an inhomogeneous broadening of <40 kHz from the dipolar coupling with powder averaging, consistent with nearest-neighbor F-F distances of 2.6–2.8 Å. This interaction is small relative to the overall linewidth and, moreover, is field independent in magnitude, contrary to the observation of a linear scaling of the experimental spectra with respect to the field. Its effects can evidently be neglected at the magnetic fields considered in this work.

Chemical shift tensors for PuF_4 have not been reported, but ^{19}F data are available for the isostructural compound CeF_4 [34], which has a tetravalent metal center with an ionic radius close to Pu^{4+}. Magnitudes of the chemical shift anisotropies of the seven fluorine sites in CeF_4 average 385 ppm, which is an order of magnitude smaller than the anisotropies indicated by Table II. The effects of the chemical shift tensor will also be ignored.

The NMR shifts of nuclei interacting with paramagnetic d- or f-electron centers have been discussed in detail by Shulman and Jaccarino [20]. Gabuda *et al.* [29] and Martel *et al.* [35] have proposed that the field-dependent anisotropic hyperfine shifts in paramagnetic tetravalent actinide systems can be approximated as a dipolar field produced by localized, unpaired electrons at the An^{4+} sites:

$$H_F = \sum_{j=1}^{N} \frac{\langle \mu_j \rangle}{r_j^3}(3\cos^2\theta_j - 1), \quad (3)$$

where r_j is the distance between the fluorine nucleus and the center, θ_j is the angle between the electronic-nuclear vector and the applied field direction, and the sum is over N nearby paramagnetic centers. The parameter $\langle \mu_j \rangle$ is the magnetic moment of the jth paramagnetic center, which in the limit of short electronic relaxation times can be approximated by its thermodynamic average [20]. To estimate the magnitude of the hyperfine field H_F, $\langle \mu_j \rangle$ was calculated for a $5f^4$ configuration according to

$$\langle \mu_j \rangle = g\mu_B J B_J(H,T), \quad (4)$$

using the appropriate Brillouin function B_J [36]. The value obtained ($\langle \mu_j \rangle = 0.038\ \mu_B$, corresponding to a hyperfine field of ~3.5 mT at $B = 7.05$ T, $T = 300$ K, with $g_J = \frac{3}{5}$ and $J = 4$) is found to be in good agreement with experimental susceptibility at 300 K in the dilute limit of a $Th_{1-x}Pu_xF_4$ ($0 \leqslant x \leqslant 1$) solid solution [37,38]. Note that the susceptibility per Pu^{4+} in pure PuF_4 is about 40% smaller than in the dilute compound. The calculated average moment was then used to compute H_F for each of the seven crystallographically distinct fluorine sites, with the sum carried out over the two nearest Pu^{4+} centers, which range between 2.230 and 2.354 Å in distance from fluorine atoms. Using these anisotropic fields, orientationally averaged powder ^{19}F spectra were independently calculated for the seven sites and summed, weighted by the multiplicity of each F site within the unit cell, with the result shown in Fig. 3(c). The program created for the spectral simulations utilized GAMMA object code for the computation of the nuclear spin dynamics [33].

As seen in Fig. 3(c), the simulated spectrum for the $5f^4$ configuration predicts a smaller linewidth than was observed experimentally, suggesting that the fluorine local magnetic fields have been underestimated. The magnitude of the computed hyperfine dipolar field can be increased by assuming an alternative electronic configuration for Pu^{4+} with a larger magnetic moment. For example, the $5f^3\ 6d^1$ configuration, with $g_J = \frac{8}{11}$ and $J = \frac{9}{2}$, gives $\langle \mu_j \rangle = 0.084\ \mu_B$ including the $6d^1$ spin in an applied field of 7.05 T and $T = 300$ K. In contrast to $5f^4$, the prediction for the $5f^3\ 6d^1$ configuration appears to overestimate the magnitude of the local field (Fig. 3(d)), which implies that an admixture of the two configurations would lead to better agreement. In particular, a linear combination of 80% ($5f^3\ 6d^1$) and 20% ($5f^4$), corresponding to a moment $\langle \mu_j \rangle = 0.075\ \mu_B$, is consistent with the experimental linewidth. This value is also close to the moment calculated for the $5f^2$ configuration assumed for UF_4 [29] and would explain the similar widths of the experimental spectra in the two compounds. However, a different value of the effective moment is determined from magnetic susceptibility measurements. In fact, PuF_4 appears to have a slightly larger effective moment $\mu_{eff} = g\sqrt{J(J+1)}\,\mu_B$ than expected for a $5f^4$ configuration ($\mu_{eff} = 2.90\ \mu_B$ instead of 2.68 μ_B) [15] but this would correspond to at most a 23% $5f^3\ 6d^1$ admixture. A similar discrepancy has been reported for UF_4, in which the moment of the electronic configuration ($5f^2$) differs from the effective moment indicated by magnetic susceptibility data [18]. Alternatively, superexchange-type antiferromagnetic correlations between Pu local moments mediated by the fluorine ligands may enhance the hyperfine field to the magnitudes implied by the ^{19}F NMR linewidths.

A purely dipolar coupling of the F nuclei to localized f electrons has no isotropic component, and therefore cannot account for a nonzero absolute shielding of the ^{19}F NMR line. The shielding observed here for PuF_4 can be estimated from the experimental ^{19}F spectra using results from Hindermann and Cornell [30] to be +1809 ppm. X-ray photoelectron spectra show evidence of a significant delocalization of one of the two $5f$ electrons in UF_4 [17], and an admixture of $4f^0 5d^1$ and $4f^1$ configurations in CeF_4 [39]. No similar experiments have been reported in PuF_4 but covalency in the Pu-F bonds and mixed valency in this compound can be expected to induce nonzero isotropic shifts in PuF_4 and related actinide tetrafluorides.

IV. CONCLUSION

Fluorine-19 NMR spectra reveal that local magnetic fields in PuF_4 and UF_4 are similar, despite the former having nominally four valence electrons and the latter two. Although ^{239}Pu is a spin-$\frac{1}{2}$ nuclide, the large magnitude of the fields generated by the metal's own valence electrons preclude its detection by NMR spectroscopy [40]. Analyses that assume purely localized $5f^4$ (for PuF_4) and $5f^2$ (for UF_4) electron configurations for the metal centers systematically underestimate the magnitudes, shifts, and anisotropy of the hyperfine field as measured by the ^{19}F NMR linewidths. Plausible modifications of the hyperfine interaction that could account for the enhanced field are admixture of higher energy electron configurations, hybridization of f-electron density with ligand orbitals, and inclusion of superexchange effects.

ACKNOWLEDGMENTS

We thank Mark Ellefson for providing information on the origin and composition of the PuF_4 stock and Nancy Washton for facilitating work at the EMSL. This work was supported in part by the U.S. Department of Energy, Office of Science, Office of Workforce Development for Teachers and Scientists (WDTS), under the Visiting Faculty Program (VFP). This material is based upon work supported by the U.S. Department of Energy Office of Science, Office of Basic Energy Sciences, Division of Chemical Sciences, Geosciences, and Biosciences, Heavy Element Chemistry program, and was performed in part in the William R. Wiley Environmental Molecular Sciences Laboratory, a DOE national scientific user facility sponsored by the Department of Energy's Office of Biological and Environmental Research and located at the Pacific Northwest National Laboratory (PNNL). PNNL is a multiprogram national laboratory operated for DOE by Battelle.

[1] G. T. Seaborg, Science **104**, 379 (1946).
[2] A. M. Boring and J. L. Smith, Los Alamos Sci. **26**, 90 (2000).
[3] J. M. Wills and O. Eriksson, Los Alamos Sci. **26**, 128 (2000).
[4] D. L. Clark, Los Alamos Sci. **26**, 364 (2000).
[5] G. Stewart, Rev. Mod. Phys. **56**, 755 (1984).
[6] E. D. Bauer, N. A. Frederick, P.-C. Ho, V. S. Zapf, and M. B. Maple, Phys. Rev. B **65**, 100506(R) (2002).
[7] F. Steglich, J. Aarts, C. D. Bredl, W. Lieke, D. Meschede, W. Franz, and H. Schäfer, Phys. Rev. Lett. **43**, 1892 (1979).
[8] H. R. Ott, H. Rudigier, Z. Fisk, and J. L. Smith, Phys. Rev. Lett. **50**, 1595 (1983).
[9] G. R. Stewart, Z. Fisk, J. O. Willis, and J. L. Smith, Phys. Rev. Lett. **52**, 679 (1984).
[10] T. T. M. Palstra, A. A. Menovsky, J. van den Berg, A. J. Dirkmaat, P. H. Kes, G. J. Nieuwenhuys, and J. A. Mydosh, Phys. Rev. Lett. **55**, 2727 (1985).
[11] M. Janoschek, P. Das, B. Chakrabarti, D. L. Abernathy, M. D. Lumsden, J. M. Lawrence, J. D. Thompson, G. H. Lander, J. N. Mitchell, S. Richmond, M. Ramos, F. Trouw, J.-X. Zhu, K. Haule, G. Kotliar, and E. D. Bauer, Science Advances **1**, e1500188 (2015).
[12] W. H. Zachariasen, Acta Crystallogr. **2**, 388 (1949).
[13] J. K. Dawson, R. M. Elliott, R. Hurst, and A. E. Truswell, J. Chem. Soc., 558 (1954).
[14] L. Asprey and R. Haire, Inorg. Nucl. Chem. Lett. **9**, 1121 (1973).
[15] W. B. Lewis and N. Elliott, J. Chem. Phys. **27**, 904 (1957).
[16] D. W. Osborne, H. E. Flotow, S. M. Fried, and J. G. Malm, J. Chem. Phys. **63**, 4613 (1975).
[17] A. Y. Teterin, Y. A. Teterin, K. I. Maslakov, A. D. Panov, M. V. Ryzhkov, and L. Vukcevic, Phys. Rev. B **74**, 045101 (2006).
[18] N. Elliott, Phys. Rev. **74**, 498 (1948).
[19] H. Alloul, Scholarpedia **10**, 30632 (2015).
[20] R. G. Shulman and V. Jaccarino, Phys. Rev. **108**, 1219 (1957).
[21] H. Crocker and H. Hopkins Jr., Conversion of Plutonium Nitrate to Plutonium Tetrafluoride via the Continuous Oxalate-Fluoride Method, Tech. Rep., General Electric Co., Hanford Atomic Products Operation, Richland, WA, 1963.
[22] Z. Szabó, J. Glaser, and I. Grenthe, Inorg. Chem. **35**, 2036 (1996).
[23] J. G. Powles and P. Mansfield, Phys. Lett. **2**, 58 (1962).
[24] A. C. Kunwar, G. L. Turner, and E. Oldfield, J. Magn. Reson. **69**, 124 (1986).
[25] R. K. Harris, E. D. Becker, S. M. Cabral de Menezes, R. Goodfellow, and P. Granger, Pure Appl. Chem. **73**, 1795 (2001).
[26] M. Hudlicky, J. Fluorine Chem. **28**, 461 (1985).
[27] D. J. Kroon, Philips Res. Rep. **15**, 501 (1960).
[28] U. Haeberlen, *High Resolution NMR in Solids*, Adv. Mag. Reson. Suppl. 1 (Academic Press, New York, 1976).
[29] S. P. Gabuda, L. G. Falaleeva, and Y. V. Gagarinskii, Phys. Status Solidi (b) **33**, 435 (1969).
[30] D. K. Hindermann and C. Cornwell, J. Chem. Phys. **48**, 4148 (1968).
[31] Differences in signs of the shift can be attributed to the specification of δ, which in some papers is the negative of the IUPAC's recommendation [25,26,30].
[32] R. Laskowski and P. Blaha, Phys. Rev. B **85**, 245117 (2012).
[33] S. Smith, T. Levante, B. H. Meier, and R. R. Ernst, J. Magn. Reson., Ser. A **106**, 75 (1994).
[34] C. Legein, F. Fayon, C. Martineau, M. Body, J.-Y. Buzaré, D. Massiot, E. Durand, A. Tressaud, A. Demourgues, O. Péron, and B. Boulard, Inorg. Chem. **45**, 10636 (2006).
[35] L. Martel, N. Magnani, J.-F. Vigier, J. Boshoven, C. Selfslag, I. Farnan, J.-C. Griveau, J. Somers, and T. Fanghänel, Inorg. Chem. **53**, 6928 (2014).
[36] J. H. Van Vleck, *The Theory of Electric and Magnetic Susceptibilities* (Clarendon Press, Oxford, 1932).
[37] J. Dawson, J. Chem. Soc., 1882 (1952).
[38] The unit given for $\chi_{Pu(IV)}$ in Table 1 of Dawson [37] appears to be in error; instead of gram (mass) ion susceptibility, we believe the correct unit is mole ion susceptibility.
[39] G. Kaindl, G. K. Wertheim, G. Schmiester, and E. V. Sampathkumaran, Phys. Rev. Lett. **58**, 606 (1987).
[40] H. Yasuoka, G. Koutroulakis, H. Chudo, S. Richmond, D. K. Veirs, A. I. Smith, E. D. Bauer, J. D. Thompson, G. D. Jarvinen, and D. L. Clark, Science **336**, 901 (2012).